POAC'25
St. John's, Newfoundland and Labrador, Canada

Proceedings of the 28th International Conference on Port and Ocean Engineering under Arctic Conditions
Jul 13-17, 2025
St. John's, Newfoundland and Labrador
Canada

Study on extreme Ice Force of Polar Vessels based on a Probabilistic Method

Boyang Jiao[1,2], Fang Li[1,2], Pentti Kujala[2,3], Li Zhou[1,2], Guangwei He[4], Shixiao Fu[1,2], Shifeng Ding[1,2]

[1] State Key Laboratory of Ocean Engineering, Shanghai Jiao Tong University, Shanghai, China
[2] School of Ocean and Civil Engineering, Shanghai Jiao Tong University, Shanghai, China
[3]Estonian Maritime Academy, Tallinn University of Technology, Tallinn, Estonia
[4] Guangzhou Shipyard International Company Limited, Guangzhou, China

ABSTRACT

In polar areas, the mechanical and physical characteristics of sea ice, combined with the inherent randomness of the interaction between ice and ships, contribute to the stochastic nature of ice forces on vessels. Aimed for the uncertainty in ice forces and the associated risks, this study employs a probabilistic method to analyze the measured ice force data. The relationship between extreme ice force and ice thicknesses was established. Design ice forces were provided based on Finish-Swedish ice class rules, and corresponding return periods were calculated to enable a quantitative evaluation of extreme ice forces the ship may encounter during its lifetime. Furthermore, a comparative analysis was conducted between the extreme ice forces of "MT Uikku" and "Agulhas II". The results indicate that the return periods of "Agulhas II" are smaller than those of "MT Uikku" under the same ice force level for "Agulhas II" operates in independent icebreaking mode and therefore faces a more harsh ice condition. The findings of this study can offer a quantitative method for risk assessment of polar vessels from a probabilistic perspective.

KEY WORDS: Probabilistic analysis; Ice force; Ice force stochasticity; Return period; Extreme ice forces

Introduction

The Arctic region is rich in oil and gas resources, with its reserves accounting for 13% of the world's oil and 30% of the world's natural gas (Gautier et al., 2009). Global warming has enhanced accessibility to Arctic shipping routes, offering shorter transit times and reduced costs compared to traditional routes like the Suez Canal (Cao et al., 2022, Shyu and Ding,

2016). However, harsh ice conditions pose critical risks to vessel structural integrity through ice-structure collisions, therefore, the study of ice forces plays a significant role in the design of polar vessels.

Ice forces on ship structures are mainly evaluated via theoretical analysis, numerical modeling, laboratory tests, and field measurements. Among these methods, field measurements yield precise data crucial for ship-ice interaction researches. Countries including Norway, China, Russia, and South Korea have accumulated extensive datasets through sustained field experiments (Wu et al., 2021). Sea ice properties vary significantly due to temperature fluctuations, salinity levels, the size of ice crystals, and their orientation, while ship-ice collisions involve dynamic mechanisms like ice fracture and fluid-solid coupling, resulting in stochastic processes (Suyuthi et al., 2012). Probabilistic analysis of ice force data, which are key factors for hull plastic deformation and cumulative damage, is vital for maintaining structural integrity.

Kheisin and Popov first studied ice forces using probabilistic methods, revealing that the ice force amplitudes follow an exponential distribution (Kheisin and Popov, 1973). Daley (1984) analyzed extreme ice forces using probabilistic models based on field measurements, providing a statistical approach of ice load fitting. Jordaan (1993) introduced a probabilistic analysis of local ice pressures, emphasizing exceedance probability models based on full-scale ship measurements. Kujala (1994) conducted statistical characterization of ice forces on ships operating in the Baltic sea, providing important insights into regional variability in ice load modelling. And with the increasing availability of full-scale ice load measurements after 2000, researchers are enabled to conduct various statistical analysis and come up with more refined probabilistic models, such as short-term statistics (Suyuthi et al., 2012), nonparametric probabilistic modeling (Suyuthi et al., 2013), and hierarchical Gaussian process models (Kotilainen et al., 2017). Recent work has emphasized uncertainty quantification of ships sailing in ice, capturing randomness in ice-structure interactions and operational variability (Shamaei et al., 2020, Li et al., 2021, Suominen et al., 2024). The above research highlights a growing emphasis on probabilistic risk quantification to advance risk-informed design frameworks for ice-going vessels (Bergström et al., 2022), integrating uncertainty management to enhance structural reliability.

This paper aims at analyzing the measured ice force data of polar vessels based on a probabilistic method, establishing the relationship between extreme ice forces and ice thickness. Return periods corresponding to different design ice forces will be calculated based on Finnish-Swedish ice class rules, providing the possible extreme ice forces that the vessel may encounter during its lifetime. Furthermore, a comparative analysis of the design ice forces and corresponding return periods for different vessels will be conducted, providing guidance and reference for the risk assessment and structural design optimization of polar vessels.

Dataset and Main Parameters of the Vessel

This paper conducts analysis based on the measured ice force data of “MT Uikku”. Kotisalo and Kujala (1999) conducted measurements of the ice forces at the bow and stern areas of the “MT Uikku” in 1998, accumulating valuable measured data for ice force research. The vessel has IA Super icebreaking capability with a design line load of 2087 kN/m at the bow area and a maximum thrust of 11.4MW. The main parameters of this vessel are shown in Table 1.

Table 1. Main parameters of MT Uikku

Length	150 m
Corresponding deadweight	15.75kt
β':normal frame angle at upper ice waterline	59.4
α: upper ice waterline angle	25.2
xd: distance from the fore side of the stem at the intersection with upper ice waterline to station under consideration	12.45

Ice force measurement was carried out by installing strain gauges at the upper, middle, and lower positions along the neutral axis of the bow and stern frames (Figure 1). The finite element method (FEM) was used to model the frame structure. Calibration coefficients were calculated to transform the measured shear strains into shear stresses, thus finally obtaining the line load data. The measurement system automatically processed and stored data every 20 minutes, documenting peak line load values along with the associated ice condition parameters.

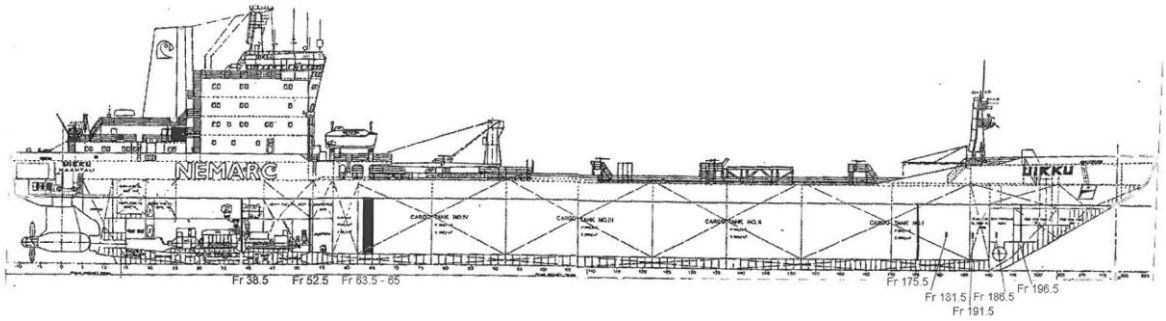

Figure 1. Schematic Diagram of the Installation Location of the Measuring Device On MT Uikku (Kotisalo and Kujala, 1999)

On April 26, 1998, the vessel, fitted with ice force measurement devices, departed from Murmansk under the guidance of the Kapitan Dranitsyn. It navigated through the Barents Sea and reached the northernmost point of Novaya Zemlja on April 29. Due to severe ice conditions at that time, the nuclear icebreaker Rossiya provided escort. After crossing the Kara Sea, Rossiya departed from the convoy, while MT Uikku and Kapitan Dranitsyn reached the Subic loading dock on May 4 and completed loading on May 8. Subsequently, both vessels returned to the Kara Sea, with Rossiya continuing its escort until it reached the Barents Sea on May 12. Upon reaching areas of light ice and open water, MT Uikku proceeded alone to Murmansk, arriving on May 13. The route of the voyage is illustrated in Figure 2.

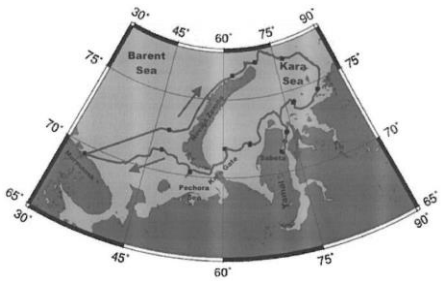

Figure 2. Route Map of the Voyage of MT Uikku (Kotisalo and Kujala, 1999)

During the navigation process, ice thickness was measured based on visual observations, and the measurement system conducts statistics on the measured ice force data and corresponding ice condition data every 20 minutes, recording the values of ice force and the maximum ice thickness. In the dataset, ice force data corresponding to trapping, port arrival/departure, and stationary conditions have been excluded from the dataset.

During the voyage, the max ice thickness during each 20-minute period was recorded in five groups: 0.1m, 0.3 m, 0.7 m, 1.2 m, and 1.5 m. Since the bow area of Uikku is the main part to collide with sea ice pieces and push them away, the ice force on the bow is larger and thereby posing threat to structural integrity. Therefore, this paper focuses on the analysis of the line loads on the bow area of Uikku, specifically at FFR2 (frame number Fr 196.5).

This paper also incorporates the icebreaker S.A. Agulhas II for comparative analysis of design ice forces and the corresponding return periods with different vessels. The main parameters of S.A. Agulhas II are listed in Table 2.

Table 2. Main parameters of S.A. Agulhas II

Length (LUI)	130 m
DUI: displacement	14 kt
β':normal frame angle at upper ice waterline	54.2 deg
α: upper ice waterline angle	33.2 deg
xd: distance from the fore side of the stem at the intersection with upper ice waterline to station under consideration	14 m

Probabilistic Method

Jordaan (1993) proposed the Event Maximum Method for probabilistic assessment of measured ice forces. This method sorts the maximum ice force values X from a series of ship-ice collision events in descending order to form an ice force sequence (X_1, X_2, ..., X_n). The exceeding probability p_e corresponding to each ice force in the sequence can be calculated using Equation (1). The relationship between the ice force and p_e is determined by plotting on the exponential probability plotting paper, where the ice force is on the horizontal axis and the Weibull plotting position ($-log(p_e)$) is on the vertical axis, as shown in Figure 3.

$$p_e = \frac{i}{n+1} \tag{1}$$

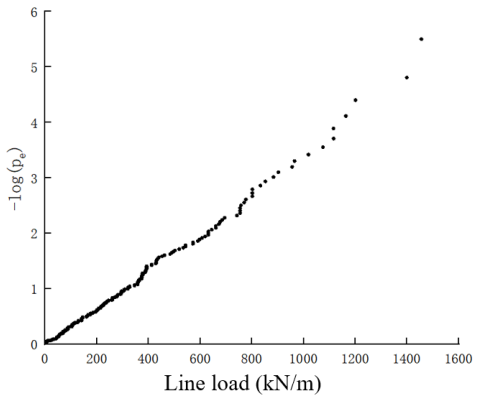

Figure 3. Illustration of line load on exponential probability plotting paper

As shown in Figure 3, it can be observed that the measured ice forces follow an approximately linear distribution. Therefore, they can be fitted using an exponential distribution, expressed as:

$$-\log(p_e(x)) = \frac{x - x_0}{\beta} \tag{2}$$

In equation (2), x_0 is the intercept of the fitted line on the horizontal axis in Figure 3, and β is the slope. The values of β and x_0 can be obtained through linear regression, establishing the relationship between the exceeding probability p_e and the ice force. To intuitively present the probability calculation results, the reciprocal of the exceeding probability can be taken to obtain the return period. The return period describes the average time interval between peak ice force events, enabling the estimation of the recurrence interval for specific ice forces of interest. This facilitates structural design and risk assessment.

Based on the Event Maximum Method, a relationship between extreme ice forces and ice thickness (h) can be established to form a predictive method. This method relies on two fundamental assumptions (Li et al., 2021): (1) Extreme ice forces from different measurement periods are independent and identically distributed (i.i.d.); (2) The tail of extreme ice forces from different measurement periods follows an exponential distribution.

During ice force measurements, different measurement periods remain independent, and the ship's navigation parameters are nearly constant, resulting in consistent ice force distributions. Assumption (2) originates from the Event Maximum Method, where the tail of extreme ice forces on the exponential probability plot exhibits an approximately linear distribution, justifying the use of an exponential distribution. Here, the top 20% of ice forces within each measurement period are assumed to represent the tail data (Shamaei et al., 2020).

To establish the relationship between ice forces and ice thickness, the parameters β and x_0 can be expressed as functions of ice thickness:

$$\beta = \theta_1 h^{\theta_2} \tag{3}$$

$$x_0 = \theta_3 h^{\theta_4} \tag{4}$$

Let $y=-log(p_e)$, the estimated ice force value $\hat{x}$ can then be expressed as:

$$\hat{x} = \theta_1 h^{\theta_2} y + \theta_3 h^{\theta_4} \tag{5}$$

Since only the top 20% of extreme ice force data from each measurement period is used for fitting, y is replaced with y' (where $y' = y + log(0.2)$), and the estimated ice force value can be expressed as:

$$\hat{x} = \theta_1 h^{\theta_2} y' + \theta_3 h^{\theta_4} \tag{6}$$

Extract and combine the top 20% of extreme ice forces from each measurement period to form a dataset. The parameters θ_1 to θ_4 are solved by minimizing the sum of squared errors E, where E is defined as:

$$E = \sum_{i}^{N} \frac{1}{2} (x_i - \hat{x}_i)^2 \tag{7}$$

In the equation, N is the total number of ice force data points in the dataset, x_i is the true ice force value, and $\hat{x}_i$ is the estimated ice force value. To minimize E, the derivatives of E with

respect to parameters θ_1 to θ_4 are set to zero. This constructs a nonlinear system consists of four equations with four unknowns. The optimized parameter values can then be obtained by solving this nonlinear system using numerical iterative methods.

Results and Discussion

Using the method proposed in this study, the extreme ice forces at the bow area of the hull were fitted. The results of θ_1 to θ_4 are listed in Table 3.

Table 3. Fitted parameters

Parameter	Value
θ_1	262.92
θ_2	0.20
θ_3	393.87
θ_4	0.71

The empirical cumulative distribution function (ECDF) curves between the ice force data and fitting results are shown in Figure 4. One can observe that the two ECDF curves exhibit the same trend of change and are nearly identical, which shows that the fitting results match the ice force data well.

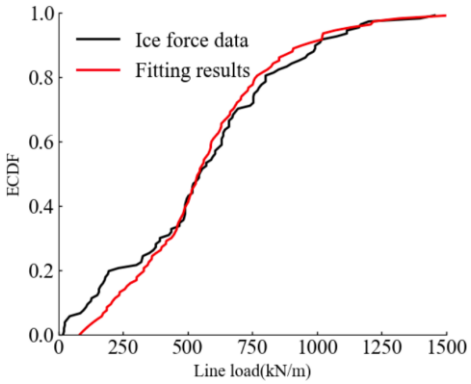

Figure 4. Comparison of ECDF between fitting results and ice force data

Meanwhile, to clearly show the changing trends between the fitting results and the raw data, Figure 5 presents a Quantile - Quantile plot. It can be observed that the scatters are basically distributed on the diagonal line (reference line), indicating that the fitting results have high accuracy. And to quantify the fitting accuracy, the coefficient of determination (R^2 score) was used for calculation. The result of R^2 score is 0.961, which means that the fitting results are in good agreement with the extreme ice forces.

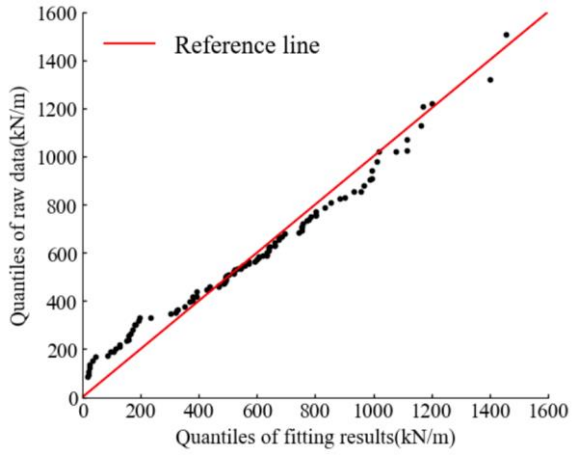

Figure 5. Q-Q plot between fitting results and the raw data

In order to translate the fitting results into a more intuitive way, the exceeding probability p_e is transformed into return period in days, and the relationship between ice force and return period under different ice thickness at bow area is shown in Figure 6. Different design line loads are also shown in Figure 6 for comparison purposes. This curve allows for the determination of return periods associated with various design ice force levels, thus providing guidance for the hull structural design process.

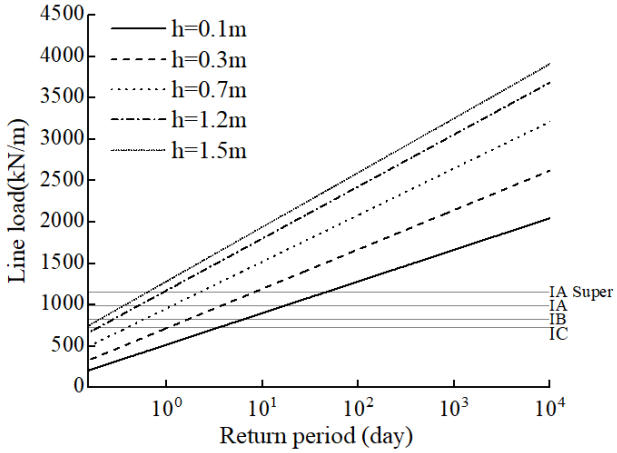

Figure 6. Relationship between line load and return period under different ice thicknesses

Furthermore, to demonstrate the methodology of this study for estimating the ice forces and corresponding return periods that the Uikku icebreaker may encounter during its lifetime, the following operating profiles of Uikku are assumed and analyzed as a case study:

Operational profile 1: The ship sails for 45 days in ice annually, with 3 days of operation in each ice thickness category (0.1, 0.2, ..., 1.5 m) during the navigation period.

Operational profile 2: The ship sails for 75 days in ice annually, with 5 days of operation in each ice thickness category (0.1, 0.2, ..., 1.5 m) during the navigation period.

Operational profile 3: The ship sails for 150 days in ice annually, with 10 days of operation in each ice thickness category (0.1, 0.2, ..., 1.5 m) during the navigation period.

Figure 7 shows the ice force-return period curves for different operatioanl profiles. Based on the results in Figure 7, the return period corresponding to the vessel's design ice force (1,160 kN/m) is approximately 37 hours, which is in accordance with Riska and Bridges (2019).

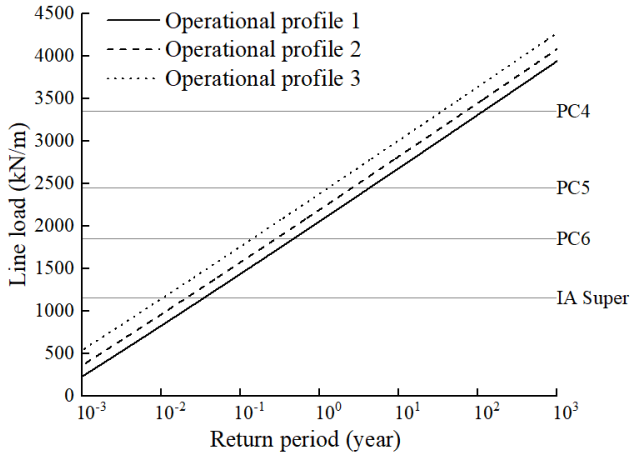

Figure 7. Relationship between line load and return period under different operational profiles

Additionally, ice forces with respect to specific return periods under different operational profiles can also be derived, as shown in Figure 8. It demonstrates that under different operational profile assumptions, the extreme ice forces the vessel may encounter within the same return period show differences in the magnitude of the values, presenting a more adaptable approach for extreme ice force prediction. This appears to be more reasonable and scientific compared to directly estimating the maximum ice forces on the hull assuming the worst ice conditions where the ship may operate (Bergström et al., 2022).

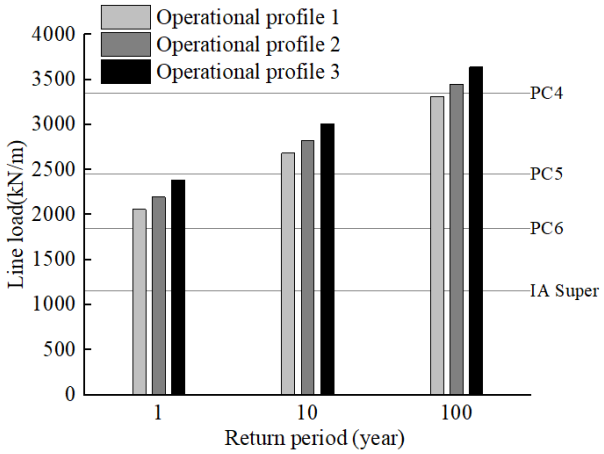

Figure 8. Predicted ice forces of different return periods under different operational profiles

Figure 9 compares the ice force-return period curves of the Uikku and Agulhas II icebreakers. For Uikku, the curve is under the assumption of operational profile 2. For Agulhas II, the return period was calculated using the extended Event Maxima method (Li et al., 2021), which incorporates both sea ice concentration and ice thickness. Here, the operational profile for Agulhas II is in accordance with operational profile 2, and the ice concentrations are assumed to be 30%, 60%, and 90%.

It can be observed that Agulhas II's return periods under all concentration conditions are shorter than those of Uikku, which aligns with Shamaei (2020), even though his analysis focused on local pressures. And the reason for this is that Agulhas II operates in independent icebreaking mode, encountering more severe sea ice conditions, whereas Uikku was assisted by another vessel most of its time, facing moderate ice conditions. Therefore, under the same return period, the ice forces experienced by Agulhas II are higher. Additionally, differences in

hull parameters and operational ice regimes during measurement (e.g., ice type, navigation speed) may also account for this discrepancy.

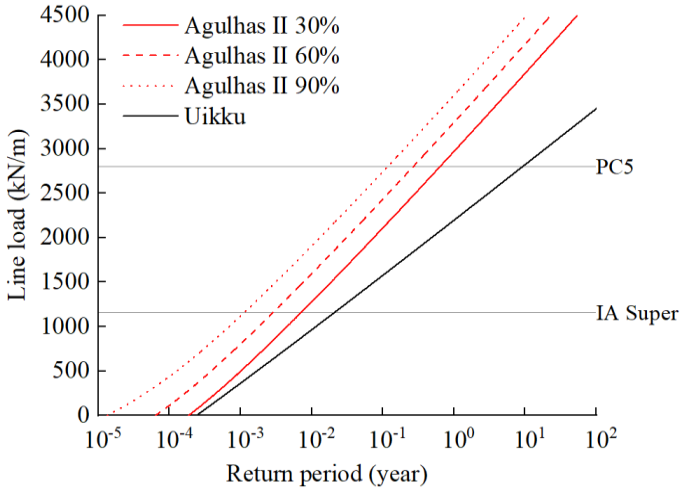

Figure 9. Comparison of return period (year) between Agulhas II and Uikku

As indicated by the results in Figure 9, the line loads corresponding to the ten - year return period for the two ships greatly surpass their design loads, and this can be attributed to several factors. Firstly, the calculation results rely on assumed operational profiles, and the actual navigation conditions may be less severe than those assumed. Secondly, during the calculation, various factors influencing ice forces, including ship speed, ice type, and ice floe size, were not taken into account. Thirdly, the ice forces calculated in Figure 9 are those corresponding to the return period of continuous navigation in polar regions. In practice, though, ships may not engage in continuous navigation for such an extended duration.

This paper presents a method for establishing the relationship between the extreme ice forces and ice thickness based on the measured ice force data of the bow area of Uikku. However, this method is not limited to this specific ship but is applicable to various types of vessels. After obtaining the measured ice force data of a certain ship, this method can be employed to rapidly establish the relationship between the extreme ice forces and ice thickness, determine the corresponding parameters, and predict the extreme ice forces.

However, this paper has limitations in the following aspects. First, the method simplifies ice conditions to a certain extent and does not comprehensively consider ship speed, ship type, ice concentration, ice floe size, etc. Second, in terms of parameter optimization, this paper adopts an optimization method based on point estimation, without taking into account the uncertainty of parameters. Future work could address this issue based on the Bayesian framework. Third, this paper does not consider how to transfer the obtained results to different ice conditions or ship types, resulting in limitations in the application of the results. Future work could consider establishing the relationship between the parameters (θ_1 to θ_4) and different ice conditions or ship types.

CONCLUSIONS

This study presents a probabilistic method to establish the relationship between extreme ice forces and ice thickness. The coefficient of determination in the Quantle-Quantle plot is 0.961, indicating that the fitting results are in good agreement with the extreme ice forces. The study also demonstrates how this method can be applied to predict ice force magnitudes acting on the bow area of hull based on return periods. Based on assumed operational profiles

as shown in Figure 8, the return period of Uikku encountering its design ice force (1160kN/m) is 37 hours. And the 1-year return period, 10-year return period and 100-year return period ice forces were also predicted. Additionally, comparison between Uikku and Agulhas II was made. Under the same assumed operational profile, return period of Agulhas II is shorter than that of Uikku because Agulhas II operates in independent icebreaking mode and thus encounters more severe ice conditions.

ACKNOWLEDGEMENTS

The author is grateful to Young Scientists Fund of National Natural Science Foundation of China (52301331), National Key Technologies Research and Development Program (Grant No. 2022YFE0107000), General Projects of National Natural Science Foundation of China (Grant No. 52171259), High-tech ship research project of Ministry of Industry and Information Technology ([2021]342), Science and Technology Commission of Shanghai Municipality Project (22DZ1204403, 23YF1419900), Foundation of State Key Laboratory of Ocean Engineering in Shanghai Jiao Tong University (GKZD010086-2).

REFERENCES

Bergström, M., Li, F., Suominen, M. & Kujala, P. 2022. A goal-based approach for selecting a ship's polar class. *Marine Structures*, 81.

Cao, Y., Liang, S., Sun, L., Liu, J., Cheng, X., Wang, D., Chen, Y., Yu, M. & Feng, K. 2022. Trans-Arctic shipping routes expanding faster than the model projections. *Global Environmental Change*, 73.

Daley, C., John, J. S. & Seibold, F. 1984. ANALYSIS OF EXTREME ICE LOADS MEASURED ON USCGC POLAR SEA. *Environmental Science*.

Gautier, D. L., Bird, K. J., Charpentier, R. R., Grantz, A., Houseknecht, D. W., Klett, T. R., Moore, T. E., Pitman, J. K., Schenk, C. J., Schuenemeyer, J. H., Sørensen, K., Tennyson, M. E., Valin, Z. C. & Wandrey, C. J. 2009. Assessment of Undiscovered Oil and Gas in the Arctic. *Science,* 324**,** 1175-1179.

Jordaan, I. J., Maes, M. A., Brown, P. W. & Hermans, I. P. 1993. Probabilistic analysis of local ice pressures. *Journal of Offshore Mechanics and Arctic Engineering,* 115**,** 83-89.

Kheisin, D. E. & Popov, Y. 1973. Ice navigation qualities of ships. *Cold Regions Research and Engineering Laboratory*.

Kotilainen, M., Vanhatalo, J., Suominen, M. & Kujala, P. 2017. Predicting local ice loads on ship bow as a function of ice and operational conditions in the Southern Sea. *Ship Technology Research,* 65**,** 87-101.

Kotisalo, K. & Kujala, P. 1999. Ice Load Measurements Onboard MT Uikku. *Measurement results from the ARCDEV-voyage to Ob-estuary.* Otaniemi: Helsinki University of Technology Ship Laboratory.

Kujala, P. 1994. ON THE STATISTICS OF ICE LOADS ON SHIP HULL IN THE BALTIC. *Environmental Science, Geography, Engineering*.

Li, F., Suominen, M., Lu, L., Kujala, P. & Taylor, R. 2021. A probabilistic method for long-term estimation of ice loads on ship hull. *Structural Safety,* 93.

Riska, K. & Bridges, R. 2019. Limit state design and methodologies in ice class rules for

ships and standards for Arctic offshore structures. *Marine Structures,* 63**,** 462-479.

Shamaei, F., Bergström, M., Li, F., Taylor, R. & Kujala, P. 2020. Local pressures for ships in ice: Probabilistic analysis of full-scale line-load data. *Marine Structures,* 74.

Shyu, W.-H. & Ding, J.-F. 2016. Key Factors Influencing the Building of Arctic Shipping Routes. *Journal of Navigation,* 69**,** 1261-1277.

Suominen, M., Kõrgesaar, M., Taylor, R. & Bergström, M. 2024. Probabilistic analysis of operational ice damage for Polar class vessels using full-scale data. *Structural Safety,* 107.

Suyuthi, A., Leira, B. J. & Riska, K. 2012. Short Term Extreme Statistics of Local Ice Loads on Ship Hulls. *Cold Regions Science and Technology,* 82**,** 130-143.

Suyuthi, A., Leira, B. J. & Riska, K. Non Parametric Probabilistic Approach of Ice Load Peaks on Ship Hulls. Proceedings of the ASME 2012 31st International Conference on Ocean, Offshore and Arctic Engineering, 2013.

Wu, G., Kong, S., Tang, W., Lei, R. & Ji, S. 2021. Statistical analysis of ice loads on ship hull measured during Arctic navigations. *Statistical analysis of ice loads on ship hull measured during Arctic navigations,* 223.